

COMPLEX OF Co(II) WITH LIGAND 2,2'-BIPYRIDINE AND ANIONIC TRIFLUOROACETATE: SYNTHESIS, PHYSICAL PROPERTY, STRUCTURAL ANALYSIS AND ITS ANTIBACTERIAL ACTIVITY

Endang Widjajanti Laksono^{1a}, Nofianti Vivi Astuti^{2a}, Isti Yunita^{3a}, and Kristian Handoyo Sugiyarto^{4a*}

Abstract: The complex containing Co(II), bipyridine (*bipy*), and trifluoroacetate (TFA) was prepared and characterized. The metal content, conductance, and TGA-DTG analysis estimate the formula of $[\text{Co}(\text{bipy})_3](\text{CF}_3\text{COO})_2 \cdot 5\text{H}_2\text{O}$. The magnetic property shows the moment of 4.2-5.3 BM which should correspond to the three unpaired electrons with the typically strong orbital contribution in cobalt(II). The UV-VIS spectral profiles indicate the three possible spin-allowed transitions of the corresponding quartet states. The characteristic vibration modes of *bipy* and TFA confirm the complex formula. The SEM photographs support the crystalline particle size, and the corresponding EDX signifies the existence of all elemental contents. The powder XRD profile has been refined according to the Le Bail method of the Rietica program, and the result suggests being a structurally monoclinic system of space group C2/c. This complex exhibits a weak inhibition against *S. aureus* and *E. coli* bacterial activity.

Keywords: Synthesis, characterization, $[\text{Co}(\text{bipy})_3](\text{CF}_3\text{COO})_2 \cdot 5\text{H}_2\text{O}$, 2,2'-bipyridine, trifluoroacetate, antibacteria.

1. Introduction

Concerning the physical properties and P-XRD, the chemistry of the divalent metal complexes such as Cu(II), Ni(II), Co(II), and Mn(II) to the six coordinated bidentate, bipyridine-*bipy* (Kusumawardani, Kainastiti & Sugiyarto, 2018; Sugiyarto, Louise & Wilujeng, 2020), and phenanthroline-*phen* (Sugiyarto *et al.*, 2017; Sugiyarto *et al.*, 2018; Sutrisno *et al.*, 2018) with counterpart anions of trifluoro methanesulfonate-triflate (CF_3SO_3) and trifluoro acetate-TFA (CF_3COO) have been much well studied. With the help of the Le Bail method of the Rietica program, the corresponding P-XRD is an acceptable refinement for producing the lattice parameters.

Regarding the medicinal aspects, the research of metal complexes seems to apply to anti-bacterial agents (e.g. Singh *et al.*, 2017; Uddin *et al.*, 2019; Ayipo *et al.*, 2021; Beyene & Wassie, 2020; Sondavid *et al.*, 2020). A possible explanation for the toxicity of the complexes has been postulated in the light of chelation theory (Singh *et al.*, 2017).

Therefore, our research in the metal complex should now consider the extra role of an anti-bacterial agent. The two types of bacteria around human life, gram-positive and gram-negative, should be considered, and so *Staphylococcus aureus* and *Escherichia coli* are selected in this research. For these reasons, the preparation of powder Co(II) containing tris(*bipy*) with TFA anion is now a challenge, not only directed to the common physical properties associated with magnetism, IR-UV-Vis spectral

properties, and PXRD, but also to the anti-bacterial activity. The results are reported in this study.

2. Experimental Methods

Chemical Materials

The main reagents, $\text{Co}(\text{NO}_3)_2 \cdot 6\text{H}_2\text{O}$, 2,2'-bipyridine, CF_3COONa , for the complex preparation, and $\text{CrCl}_3 \cdot 6\text{H}_2\text{O}$, $\text{Fe}(\text{NO}_3)_3 \cdot 9\text{H}_2\text{O}$, $\text{CuCl}_2 \cdot 2\text{H}_2\text{O}$, $\text{Ni}(\text{NO}_3)_2 \cdot 6\text{H}_2\text{O}$, $\text{Co}(\text{NO}_3)_2$, $\text{CuSO}_4 \cdot 5\text{H}_2\text{O}$, NH_4Cl , and KCl , for the conductivity measurement, were purchased from Aldrich-Sigma, and directly used without special treatment. Meanwhile, the Nutrient agar, Nutrient Broth, *Chloramphenicol*, bacteria *Staphylococcus aureus*, and bacteria *Escherichia coli*, for anti-bacterial measurement, were obtained from the laboratory of the Department of Biology, Yogyakarta State University.

Preparation of The Complex

The Co(II) complex of tris-bipyridine was prepared according to the anionic replacement reaction as follows. To a warmed ethanolic solution of *bipy* (0.468 g; 3 mmol, ~ 4 mL), an aqueous solution of $\text{Co}(\text{NO}_3)_2$ (0.291 g; 1 mmol, ~ 3 mL) was added. The mixture was filtered and the aqueous solution of CF_3COONa in excess (0.544 g; 4 mmol, ~ 3 mL) was added whereupon the dully greenish precipitate produced on reducing volume and scratching. It was filtered, washed with a minimum of cold water, dried in aeration, and stored in a desiccator. The preparation of the powder complex was separately done three times for reproducibility.

Authors information:

^aDepartment of Chemistry Education, Universitas Negeri Yogyakarta, Yogyakarta 55281, INDONESIA. Email: endang_widjajanti@uny.ac.id¹; nofiantivivi1011@gmail.com²; isti_yunita@uny.ac.id³; sugiyarto@uny.ac.id⁴

*Corresponding Author: sugiyarto@uny.ac.id

Received: March 25, 2023

Accepted: September 8, 2023

Published: June 30, 2024

Physical Measurements

Magnetic Moment.

The MSB of Auto Sherwood Scientific 240V-AC calibrated with $\text{CuSO}_4 \cdot 5\text{H}_2\text{O}$ was applied to measure the mass magnetic susceptibility (χ_g) of the complex. The powder of the complex was packed tightly in the Gouy tube. The difference in mass without and with (electro-) magnet reflecting the mass magnetic susceptibility was then recorded. It was converted into molar magnetic susceptibility (χ_M), and then to arrive at the corrected molar magnetic susceptibility (χ_M'), the corrected for diamagnetism of Pascal's constant was applied (Bain & Berry, 2008; Dalal, 2017). The effective magnetic moment (μ_{eff}) was obtained by the application of the general relationship, $\mu_{\text{eff}} = 2.828 \sqrt{\chi_M' \cdot T}$ BM at temperature T of the sample (Pathshala, 2021; LibreTexts™, 2021; Lancashire, 2021).

UV-Vis electronic and Infrared spectra.

A spectrophotometer model of Pharmaspec UV 1700 was used to administer the UV-VIS electronic spectra. For the solid, the powder was spread on a white circle filter paper fitted to the cell holder and it was then recorded at 300-800 nm. An Infrared Spectrophotometer of the FTIR-ABB MB3000 model was used to record the IR spectrum of the complex. The powdered complex, which was mixed with KBr, was pressed on the cell holder for recording at 400-4000 cm^{-1} .

Metal content and Electrical conductance.

An AAS of the PinAAcle 900T Perkin Elmer model was used to record the metal content. A conductometer of the Lutron CD-4301 model was used to estimate the conductance property of the complex. An aqueous solution of KCl (1 M) at 25 °C was applied in calibrating this instrument prior to use, and some known ionic solutions, $\text{CrCl}_3 \cdot 6\text{H}_2\text{O}$, $\text{Fe}(\text{NO}_3)_3 \cdot 9\text{H}_2\text{O}$, $\text{CuCl}_2 \cdot 2\text{H}_2\text{O}$, $\text{Ni}(\text{NO}_3)_2 \cdot 6\text{H}_2\text{O}$, $\text{Co}(\text{NO}_3)_2$, $\text{CuSO}_4 \cdot 5\text{H}_2\text{O}$, and NH_4Cl were also administered for comparison.

TGA-DTA (Thermogravimetric and Differential Thermal Analysis).

The loss of the molecule of water and the decomposition of the complex was performed on the Diamond Perkin Elmer Instruments, and the simultaneous TGA-DTG were obtained by a NETZSCH STA 409C/CO thermal analyzer model with the rate of 10 °C/min.

Powder X-Ray Diffraction.

A Benchtop Diffractometer of Rigaku Miniflex 600 40 kW 15 mA (with $\text{CuK}\alpha$, $\lambda = 1.5406 \text{ \AA}$) was used to record the diffractogram of the complex. The sample was spread on a special glass plate and set on the cell holder. The diffractogram was then recorded in a scan mode at 2–90 degrees of 2θ within the interval of 0.04 steps per 4 sec for 2 h. It was then refined following the Le Bail method of the Rietica program within 10-60 degrees of 2θ within 30 cycles.

Determination of Antibacterial Property.

The antibacterial properties of the complex were tested against *Staphylococcus aureus* (ATCC 25924) as gram-positive type and *Escherichia coli* (ATCC 35218) as gram-negative type according to agar disk-diffusion method by the media of Nutrient Agar (NA) and Nutrient Broth (NB). Chloramphenicol was applied as the standard antibacterial agent (positive control), with water as the negative control. Various concentrations of the complex were performed at 125, 250, 500, and 1000 $\mu\text{g}/\text{mL}$. The observation of the inhibition zone (in mm) was done every 3 hours during 24 hours of the incubation. The diameter of the inhibition zone was recorded and measured using a caliper (accuracy 0.02 mm) on 3 sides of the sample (Kani et al., 2016; Balouiri et al., 2016).

3. Results and Discussion

Determining the Chemical Formula of the Complex

The complex should primarily contain $\text{Co}(\text{II})$, *bipy*, TFA, and likely molecules of H_2O . The ionic property of the complex is characterized by measuring the corresponding equivalent electrical conductance. It was estimated by comparing it with other known simple compounds, and the results are shown in **Table 1**. It falls in the range of the known ionic simple compounds consisting of three ions per molecule and therefore the stoichiometric formula, $[\text{Co}(\text{bipy})_n](\text{CF}_3\text{COO})_2 \cdot x\text{H}_2\text{O}$, where $n = 3$, is then proposed for the complex. This suggests that the formula of the complex indicates no coordinated anion is involved.

Table 1. The equivalent electrical conductance of the complex and several simple known compounds in an aqueous solution

Salts	Conductance, Λ_c , ($\Omega^{-1} \text{cm}^2 \text{mol}^{-1}$)	The ratio number of cations to anions	The number of ions per molecule
CuSO ₄ ·5H ₂ O	84.5614	1:1	2
NH ₄ Cl	125.3755	1:1	2
CuCl ₂ ·2H ₂ O	172.0782	1:2	3
Ni(NO ₃) ₂ ·6H ₂ O	178.2714	1:2	3
Co(NO₃)₂·6H₂O	226.3955	1:2	3
Fe(NO ₃) ₃ ·9H ₂ O	285.2816	1:3	4
CrCl ₃ ·6H ₂ O	436.4573	1:3	4
[Co(<i>bipy</i>)_n](CF₃COO)₂·xH₂O	217.2518	1:2	3

As shown in Fig. 1 and Table 2, the loss of mass of about 11.64 % (ca. 11.61 %, giving an error of 0.25%) in the first stage, up to 90°C, is believed to be the loss of water molecule (Paswan et al., 2019), corresponding to 5.5H₂O. While the remaining stages are not analyzed in detail, it seems the DTG curve suggests that the ligand-*bipy* is lost in three stages (Czakis-Sulikowska & Czylkowska, 2003), and the residue at above 540°C (17.78%) is likely believed to be the slow conversion of metal oxides as observed for the different complexes of Co(II) (Chaudhary et al., 2015; Mir & Ashraf, 2021).

In addition, the metal content Co, being obtained from the atomic absorption spectral data, with 7.00 % (ca. 6.91 %, giving an error of 1.3%) confirms the proposed formula of [Co(*bipy*)₃](CF₃COO)₂·5.5H₂O.

Table 2. The proposed formula of the complex estimated by the hydrate and metal content estimated by TGA and AAS data showing the percentage calculated error figures (in brackets *)

Proposed complex	H ₂ O content (%)		Co content (%)	
	calculated	TGA-DTG	calculated	AA S
[Co(<i>bipy</i>) ₃](CF ₃ COO) ₂ ·4.5H ₂ O	9.70 (20.0*)		7.06 (0.85*)	
[Co(<i>bipy</i>) ₃](CF ₃ COO) ₂ ·5H ₂ O	10.67 (9.09*)		6.98 (0.28*)	
[Co(<i>bipy</i>)₃](CF₃COO)₂·5.5H₂O	11.61 (0.25*)	11.6	6.91 (1.30*)	7.0
[Co(<i>bipy</i>) ₃](CF ₃ COO) ₂ ·6H ₂ O	12.53 (7.10*)		6.84 (2.34*)	

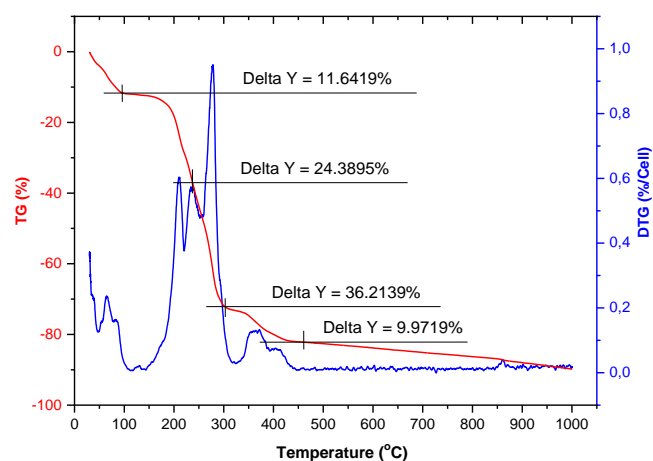


Figure 1. The TGA-DTG of [Co(*bipy*)₃](CF₃COO)₂·xH₂O at 30-1000°C

Magnetism

For the magnetic susceptibility measurement, the three samples of the Co(II) complex were prepared separately to confirm the reproducibility. The magnetic susceptibility data as shown in Table 3, produce the magnetic moments of 4.3-5.2 BM, being comparable to other reported data, e.g. 5.14 BM (Mihsen & Shareef, 2018), and 4.7 BM (Hassoon et al., 2020). The moments are significantly higher than the magnetic moment due to the spin only for the 3 unpaired electrons ($\mu_s = 3.87 \text{ BM}$) in the high-spin 3d⁷ of Co(II), which is not unusual for the strong orbital contribution to the magnetism observed in this octahedral complex (Pathshala, 2021; LibreTexts™, 2020; Lancashire, 2020; Dalal, 2017).

Table 3. The magnetic moment of [Co(*bipy*)₃](CF₃COO)₂·5.5H₂O

Sample	T (K)	χ_g (cgs)	μ_{eff} (BM)
1	291	1.27112 x 10 ⁻⁵	4.91
2	291	9.41033x 10 ⁻⁶	4.20
3	291	1.50319 x 10 ⁻⁵	5.35

Electronic Spectrum

The magnetic data of high-spin octahedral Co(II) in the complex suggests having the triply ground state of the quartet, ⁴T_{1g}(F). Therefore, following the Tanabe-Sugano diagram (Dalal, 2017), the main spin-allowed transitions of ⁴T_{1g}(F) → ⁴T_{2g}(F), ⁴T_{1g}(F) → ⁴A_{2g}(F), and ⁴T_{1g}(F) → ⁴T_{1g}(P), might assign to the corresponding UV-VIS spectral profiles. As displayed in Fig. 2, the powder spectrum exhibits an indicative of those transitions, the first broad ligand field band centered at ~15850 cm⁻¹ (ν₁), the second shoulder at ~18750 cm⁻¹ (ν₂), and the third shoulder at ~20500 cm⁻¹ (ν₃), respectively; the third ligand field band might overlap with the M-L charge transfer.

In the solution, the spectrum does not well resolve the ligand field bands (Fig. 2), and only their shoulders appear. The intensities, however, are to be very low with the extinction coefficient of 3.66-11.15 Lmol⁻¹ cm⁻¹, supporting the octahedral geometry of the complex (Lancashire, 2021), which is consistent with the magnetic data.

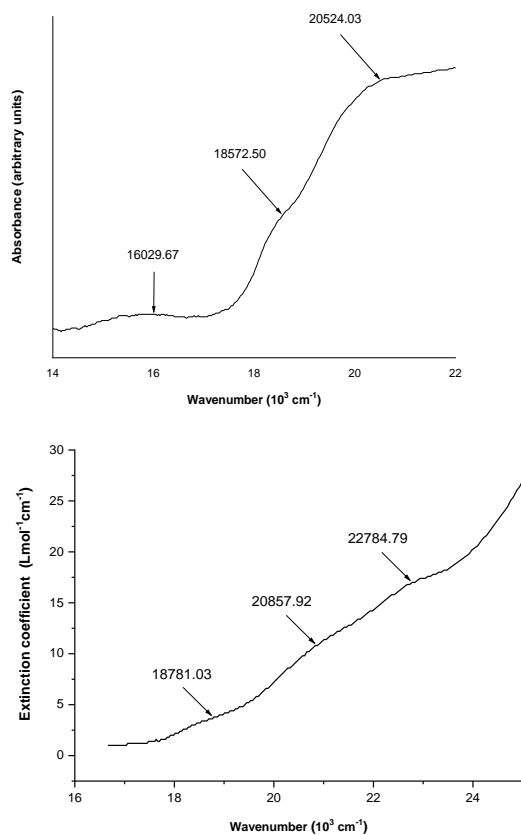


Figure 2. The electronic spectra of the powder (above), and in an aqueous solution, 0.005 M (below) for $[Co(bipy)_3](CF_3COO)_2 \cdot 5.5H_2O$

The Infrared Spectra

The infrared spectrum of the complex, $[Co(bipy)_3](CF_3COO)_2 \cdot 5.5H_2O$, is displayed in Fig. 3, together with that of $CF_3COONa \cdot 4H_2O$, and thus allowing the direct assignment. The broadband (Fig. 3A-red full line) at about 3399 cm^{-1} is likely due to the symmetric-/anti symmetric- stretching modes of -OH

of the H_2O lattice as indicated in the TGA-DTG data (Fig. 1) for the complex. This is comparable as observed at 3398 cm^{-1} by Abebe, Kendie, & Tigineh (2022), and at $\sim 3441\text{ cm}^{-1}$ by Shad et al. (2011), even though Kumar et al. (2014) reported that to be C-C aromatic at 3430 cm^{-1} .

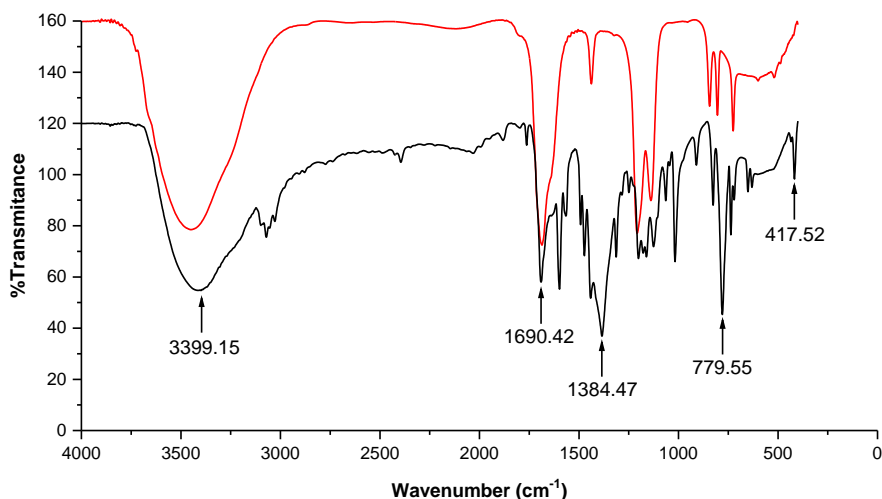


Figure 3. The IR Spectra of $[Co(bipy)_3](CF_3COO)_2 \cdot 5.5H_2O$ (black) and CF_3COONa (red) [Note: Relative transmittance (in %) only significant for each spectrum]

A multiplet band centered at about $3028\text{--}3097\text{ cm}^{-1}$ might be attributed to the mode of C-H of pyridine rings, being comparable to those of $3051\text{--}3068\text{ cm}^{-1}$ (Chen et al., 2006; Tosonian et al., 2013), and of 3100 cm^{-1} (Sugiyarto et al., 2020). The typical mode of bipyridine at $\sim 1598\text{ cm}^{-1}$ is likely attributed to being $\nu_{\text{C}=\text{C}}$ aromatic as observed by Mihsen & Shareef (2018) at 1579 cm^{-1} . The mode at $\sim 1384\text{ cm}^{-1}$ is to be $\nu_{\text{C}-\text{N}}$ vibration as observed at $\sim 1342\text{ cm}^{-1}$ by Sutrisno et al. (2018). That mode at $\sim 1441\text{ cm}^{-1}$ seems to be $\nu_{\text{C}-\text{N}}$ vibration, being close to 1449 cm^{-1} , while that at $\sim 1177\text{ cm}^{-1}$ might be due to $\nu_{\text{C}-\text{C}}$ ring as it is relatively close to 1257 cm^{-1} (Abebe, Kendie & Tigineh, 2022).

For the TFA, the very strong-sharp peaks at about 1690 and 1017 cm^{-1} are assigned due to the mode of vibrations $\nu_{(\text{C}=\text{O})}$ and $\nu_{(\text{C}-\text{O})}$, respectively, which is the same order observed by Skyranou et al. (2010) and Suzuki et al. (1978) at 1669 cm^{-1} , and by Osowole et al. (2008) at $1192\text{--}1102\text{ cm}^{-1}$. Meanwhile, mode at about 1442 cm^{-1} might be due to $\nu_{(\text{C}-\text{C})}$ as proposed by Abdelhak et al. (2014). The sharp mode of about 1670 cm^{-1} seems attributed to the C=O vibration as that observed for the sodium TFA (Fig. 3B), which was

also reported at 1669 cm^{-1} by Skyranou et al. (2010). The stretching mode at ~ 750 and 848 cm^{-1} are assigned as the asymmetry and symmetry deformation of CF_3 , respectively (Kusumawardani et al., 2017), as well as in the sodium TFA. Zhou et al. (2003) reported that the asymmetric deformations of CF might fall in the region of $500\text{--}625\text{ cm}^{-1}$, whereas the mode of 700 cm^{-1} is to be the bending vibration of O=C-O. The relatively tiny sharp mode at 417 cm^{-1} is likely evidence of the Co-N bond (Lever ABP & Mantovani, 2011).

SEM, EDX, and Powder XRD

The particle size as shown in the image of SEM, Fig. 4 (a), might consider the powder complex to be a relatively bulky polycrystalline rather than the amorphous type, and the presence of all the main elemental contents (carbon, nitrogen, oxygen, fluorine, and cobalt) is confirmed by the EDX-graph in Fig. 4 (b). The corresponding diffractogram profile (Fig. 5) shows no broad but sharp peaks, supporting no amorphous powders.

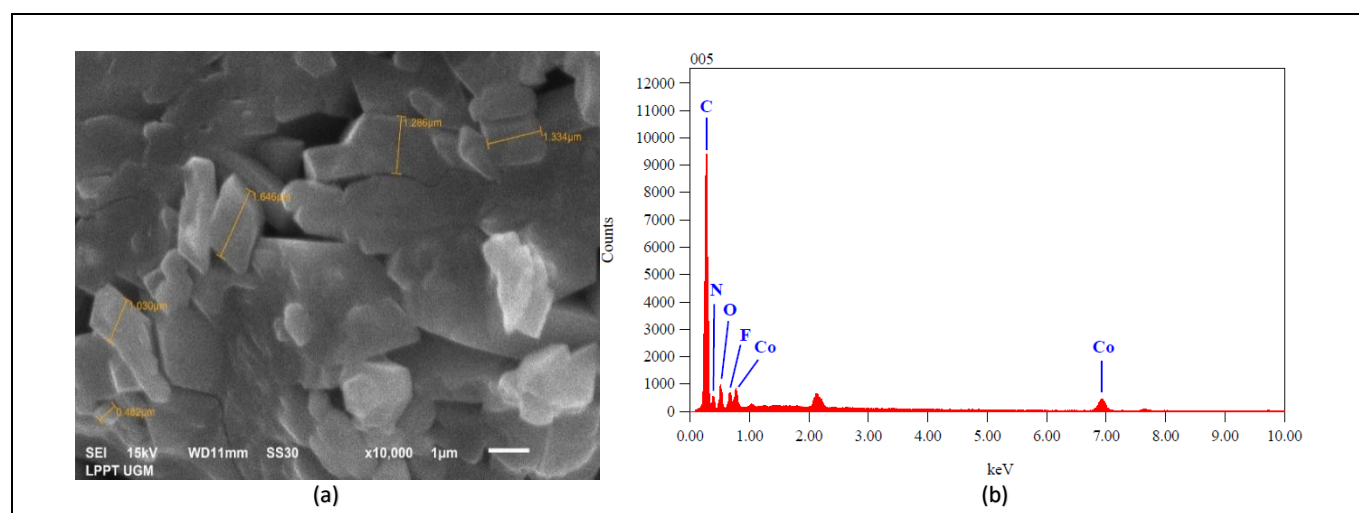


Figure 4. SEM photograph of $[\text{Co}(\text{bipy})_3](\text{CF}_3\text{COO})_2 \cdot 5.5\text{H}_2\text{O}$ at a magnification of $10,000 \times$ showing crystal size (a) and EDX showing elemental content (b)

The lattice parameters of the powder $[\text{Co}(\text{bipy})_3](\text{CF}_3\text{COO})_2 \cdot 5.5\text{H}_2\text{O}$ were deduced from the results of the refinement of the diffractogram following the method of Le Bail with the program of Rietica, as displayed in Fig. 5 and **Table 4**. For comparison, the cell parameters of two single crystals (Yao, Ma, & Yao, 2005; Benabdallah et al., 2019) and a PXRD of cationic $[\text{Co}(\text{bipy})_3]^{2+}$ (Sugiyarto, Kusumawardani, & Wulandari, 2018) are presented.

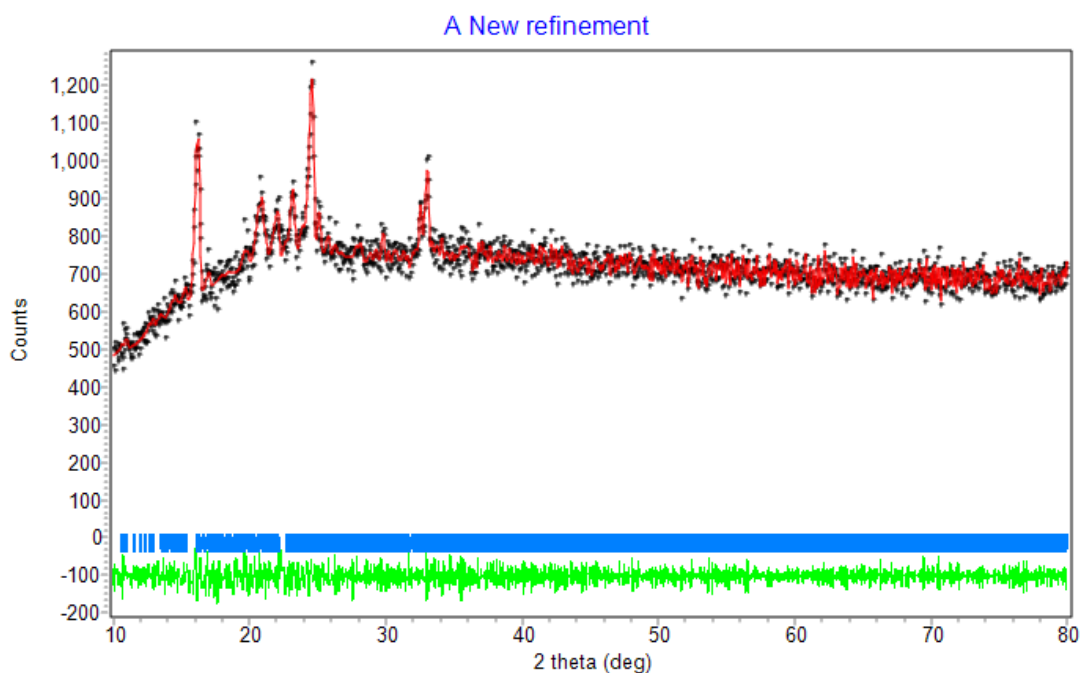


Figure 5. P-XRD profile of $[\text{Co}(\text{bipy})_3](\text{CF}_3\text{COO})_2 \cdot 5.5\text{H}_2\text{O}$ (black), the monoclinic symmetry of C2/c due to the refinement (red), the position of 2θ (blue), and the difference between the two (green)

Table 4. Lattice parameter data of $[\text{Co}(\text{bipy})_3]\text{X}_2^{a-d}$

$[\text{Co}(\text{bipy})_3]\text{X}_2$	$\text{X}_2 = (\text{TFA})_2 \cdot 5.5\text{H}_2\text{O}^a$	$\text{X}_2 = (\text{CF}_3\text{SO}_3)_2 \cdot 8\text{H}_2\text{O}^b$	$(\text{C}_9\text{H}_5\text{N}_4\text{O})_2^c$	$(\text{ClO}_4)_2^d$
Symmetry	Monoclinic	Monoclinic	Monoclinic	Monoclinic
Space group	C2/c	C2/c	C2/c	C12/c1
Z	4	4	4	4
a (Å)	28.5411	28.3991	22.335(4)	17.538(4)
b (Å)	13.9234	13.8964	10.9454(17)	10.897(2)
c (Å)	22.2933	22.2896	18.721(3)	16.078(3)
α (°)	90.0000	90.0000	90.0000	90.0000
β (°)	86.8185	86.8444	110.691(5)	91.01(3)
γ (°)	90.0000	90.0000	90.0000	90.0000
Volume (Å ³)	8845.4824	8783.2304	4281.4(12)	3072.2
<i>The Figure of Merits</i>				
R_p	2.30	2.77	-	-
R_{wp}	3.52	6.24	-	-
R_{exp}	4.10	1.63	-	-
GOF	0.7366	14.79	-	-
$R-F_{Bragg}$	0.04	0.02	-	-

[^aThis work, ^b Sugiyarto, Kusumawardani & Wulandari, 2018; ^c Yao, Ma, & Yao, 2005; ^d Benabdallah et al., 2019]

As shown in **Figure 5**, the red line of the refinement passes through almost all the black points of experimental XRD data at the blue bar space group and symmetry model. The green line reflecting the difference of the model and the experimental data seems to be flat-linear. In addition, the figure of merits is to be acceptable-low. For these reasons, the refinement should satisfy the model, and hence it can be concluded that the powdered complex follows the C2/c space group, with lattice parameters, $a = 28.5411 \text{ \AA}$, $b = 13.9234 \text{ \AA}$, $c = 22.2933 \text{ \AA}$, $\alpha = 90^\circ$, $\beta = 86.8185^\circ$, $\gamma = 90^\circ$, $V = 8845.4824 \text{ \AA}^3$, and $R-F_{Bragg} = 0.04$.

The Antibacterial Activity Test

Concerning the antibacterial agent, the complex was tested against *Staphylococcus Aureus* (S.A) and *Escherichia Coli* (E.C) bacteria with chloramphenicol as a positive control according to agar disc-diffusion method in Nutrient Agar (NA) and Nutrient Broth (NB) or diffusion assay procedures (Balouiri et al., 2016; Davis & Stout, 1971). They represent the two types, gram-positive and gram-negative, respectively, which are pathogenic and easily found in humans. All numeric data of the concentration of the complex, and the zone diameter of the clear inhibition (in mm) with time (in hours) are summarized and depicted graphically in **Fig. 6** and **Fig. 7**.

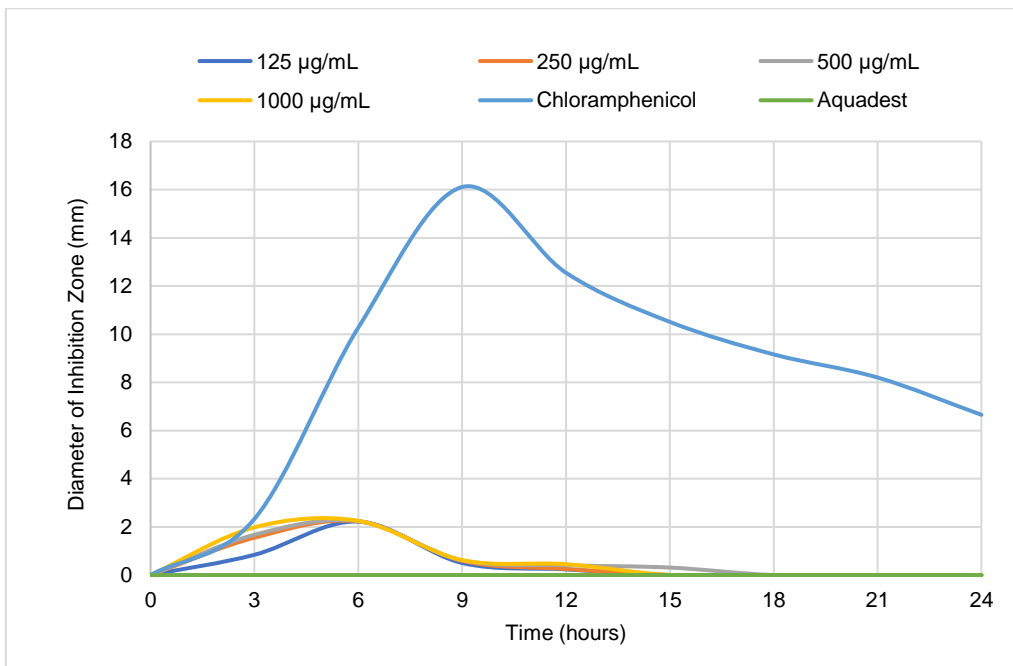


Figure 6. Graph of the zone diameter of the clear inhibition (in mm) at various concentrations of the complex against the time for the *S. aureus* activity

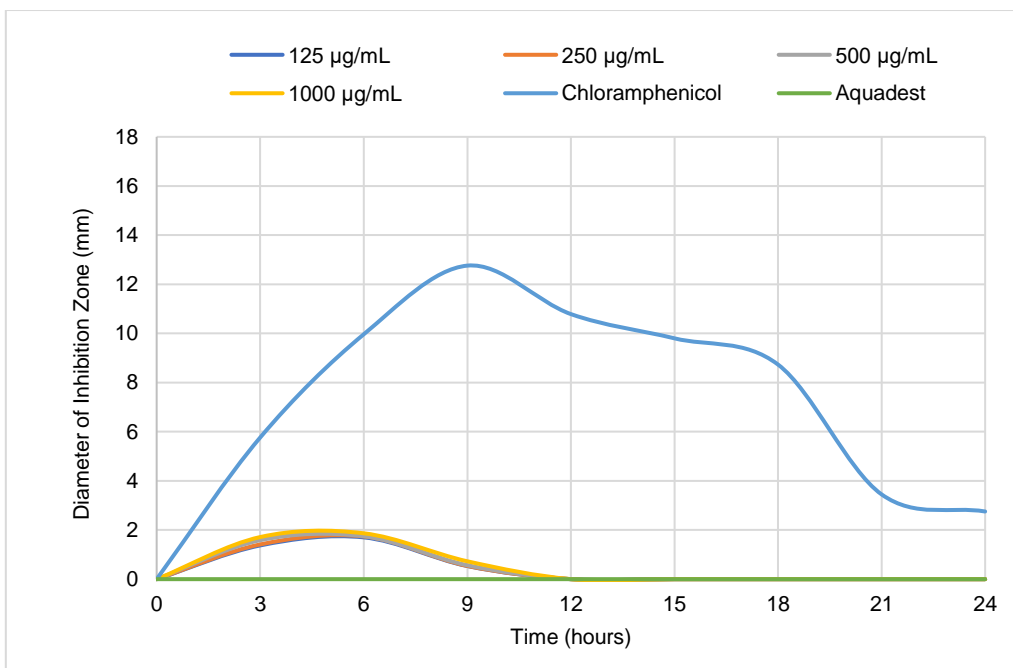


Figure 7. Graph of the zone diameter of the clear inhibition (in mm) at various concentrations of the complex against the time for the *E. coli* activity

Following the Kolmogorov-Smirnov test, it was found that the diameter data of the clear inhibition zone is not normally distributed ($p = 0.000$; $p < 0.05$), and based on the Levene’s Test, it is not homogeneous ($p = 0.000$; $p < 0.05$). According to the next non-parametric tests, Kruskal-Wallis and Mann-Whitney tests, it can be concluded that the complex in all variant concentrations

falls statistically into ‘no different’ category ($p = 0.000$; $p < 0.05$), and a weak antibacterial agent (Davis & Stout, 1971; Rastina, Sudarwanto, & Wientarsih, 2015). **Table 5** shows the average inhibition zone of the complex at the optimum time of hour six and that of the positive-negative control, chloramphenicol-aquadest, at hour nine.

Table 11. Diameter of the average inhibition zone at various concentrations of the complex and the antibacterial power

Concentration of the complex	Diameter of the average inhibition zone (mm)		Category of Antibacterial Power
	Due to <i>S. aerous</i>	Due to <i>E. coli</i>	
125 µg/mL	2.22	1.70	Weak
250 µg/mL	2.23	1.74	Weak
500 µg/mL	2.24	1.75	Weak
1000 µg/mL	2.25	1.87	Weak
Aquadest	0.00	0.00	None
Chloramphenicol	16.11	12.76	Strong

In the light of chelation theory, the ligand *bipy* may be considered to be highly stable; however, the high-spin complex of Co(III) suggests that the tris-ligand provides significantly a weak ligand field strength, and this might cause a weak antibacterial agent, as quite recently observed for $[Mn(bipy)_3](CF_3SO_3)_2$ (Sugiyarto et al., 2023).

4. Conclusion

The powdered compound of $[Co(bipy)_3](CF_3COO)_2 \cdot 5.5H_2O$ has been isolated and strongly confirmed by AAS, DTG-TGA, conductance, magnetism, UV-VIS, and IR spectral properties. The presence of elemental content, except for hydrogen, is confirmed by the EDX.

The corresponding cell parameters have been reviewed by Le-Bail refinement to the P-XRD diffractogram, which is found as fit as monoclinic symmetry of the C2/c space group. Its antibacterial activity against *S. aureus* and *E. coli* bacteria has been studied to show the inhibition of bacterial growth in the weak category.

5. Acknowledgement

Authors greatly acknowledge the Faculty of Mathematics and Natural Sciences, Yogyakarta State University, for the financial support with a contract number of /4.57/UN/34.21/PT.01.03/2021

6. References

- Abdelhak, J., Cherni, S. N., & Zid, M. F. (2014). Synthesis, characterization, and crystal structure of new cobalt(III) complex: [Tris(1,10-phenanthroline-κ2N,N') cobalt(III)] trinitrate monohydrate $[Co(C_{12}H_8N_2)_3](NO_3)_3 \cdot H_2O$, *Mediterranean Journal of Chemistry*, 3 (1), 738–745. DOI: 10.13171/mjc.2014.26.03.22.
- Abebe, A., Kendie, M., & Tigineh, G.T. (2022). Mono-and Binuclear Cobalt(II) Mixed Ligand Complexes of 2,2'-Bipyridine and Ethylenediamine: Synthesis, Characterization and Biological Application. *Biointerface Research in Applied Chemistry*, 12, 1962-1973. <https://doi.org/10.33263/BRIAC122.19621973>
- Ayipo, Y. O., Osunniran, W. A., Badeggi, U. M., Saheed, I. O., Jimoh. A. A., Babamale, H. F., & Olaide, E. O., (2021). Synthesis, characterization and antibacterial study of Co(II) and Cu(II) complexes of mixed ligands of piperazine and diclofenac. *JOTCSA, Journal of the Turkish Chemical Society Chemistry*, 8(2):633–50. DOI: <https://doi.org/10.18596/jotcsa.8985235>
- Bain, G. A., & Berry, J. F. (2008). Diamagnetic Corrections and Pascal's Constants. *Journal of Chemical Education*, 85(4): 532-536. DOI:10.1021/ed085p532.
- Balouiri, M., Sadiki, M., & Ibsouda, S. K. (2016). Methods for in vitro evaluating antimicrobial activity: A review. *Journal of Pharmaceutical Analysis*, 6(2), 71–79. <https://doi.org/10.1016/j.jpha.2015.11.005>
- Benabdallah, J., Setifi, Z., Setifi, F., Boughzala, H., & Titi, A. (2019). Crystal structure of tris(2,2'-bipyridine)cobalt(II) bis(1,1,3,3-tetracyano-2-ethoxypropenide). *Acta Crystallographica Section E: Crystallographic Communications*, 75(2), 142–145. doi:10.1107/s2056989018018261
- Beyene, B. B., & Wassie, G. A. (2020). Antibacterial activity of Cu(II) and Co(II) porphyrins: role of ligand modification. *BMC Chemistry* 14, 51:1-8 <https://doi.org/10.1186/s13065-020-00701-6>
- Chaudhary, R. G., Juneja, H. D., Pagadala, R., Gandhare, N. V. & Gharpure, M. P. (2015). Synthesis, characterization, and thermal degradation behavior of some coordination polymers by using TG–DTG and DTA techniques. *Journal of Saudi Chemical Society*, 19(4), 442–453. doi:10.1016/j.jscs.2014.06.002]]
- Chen, H., Xu, X.-Y., Gao, J., Yang, X.J., Lu, L. D., & Wang, X. (2006). Study on crystal structure of $[Ni(phen)_3](ClO_4)_2$. *Acta Physico-Chimica Sinica*, 22 (7), 856–859. DOI:10.3866/PKU.WHXB20060717
- Czakis-Sulikowska, D., & Czykowska, A. (2003). Thermal and other properties of complexes of Mn(II), Co(II) and Ni(II) with 2,2'-bipyridine and trichloroacetates. *Journal of Thermal Analysis and Calorimetry*, 74, 349–360 (2003). <https://doi.org/10.1023/A:1026371029185>
- Dalal, M. A. (2017). Textbook of Inorganic Chemistry-Volume 1 (First Edition). CHAPTER 9. *Magnetic Properties of Transition Metal Complexes*. India: Dalal Institute, pp.342-386.
- Davis, W. W., Stout, T. R.(1971). Disc plate method of microbiological antibiotic assay. I. Factors influencing variability and error. *Applied Microbiology*, 22(4), 659-65. doi:

- 10.1128/am.22.4.659-665.1971. PMID: 5002143; PMCID: PMC376382.
- Hassoon, A. A., Harrison, R. G., Nawar, N., Smith, S. J., & Mostafa, M. M. (2020). Synthesis, single crystal X-ray, spectroscopic characterization and biological activities of Mn²⁺, Co²⁺, Ni²⁺ and Fe³⁺ complexes. *Journal of Molecular Structure*, *1203*(3), 127240-127264. doi:10.1016/j.molstruc.2019.12724.
- Kani, I., Atlier, Ö., & Güven, K. (2016). Mn(II) complexes with bipyridine, phenanthroline and benzoic acid: Biological and catalase-like activity. *Journal of Chemical Sciences*, *128*(4), 523–536. DOI 10.1007/s12039-016-1050-z.
- Kumar, S. P., Suresh, R., Giribabu, K., Manigandan, R., Munusamy, S., Muthamizh, S., & Narayanan, V. (2014). Microwave synthesis of Tris-(1,10-phenanthroline)Manganese(II) complex and its electrochemical sensing property of catechol. *International Journal of ChemTech Research*, *6* (6), 3280-3283.
- Kusumawardani, C., Kainastiti, F., and Sugiyarto, K. H. (2018). Structural Analysis of Powder Complex of Cu(bipy)₃(CF₃SO₃)₂(H₂O)_x (x = 0.5, 1). *Chiang Mai Journal of Science*, *45*(4), 1944-1952. <http://epg.science.cmu.ac.th/ejournal/>
- Kusumawardani, C., Permasari, L., Fatonah, S. D., & Sugiyarto K. H. (2017). Structural Analysis of Powder Complex of Tris(1,10-phenanthroline)copper(II) Trifluoromethane Sulfonate Dihydrate, *Oriental Journal of Chemistry*, *33*(6), 2841-2847. <http://dx.doi.org/10.13005/ojc/330617>
- Lancashire, R. J. (2021). LibreTexts Chemistry: *Selection Rules for Electronic Spectra of Transition Metal Complexes*, Last updated, Jan 30, 2023. [https://chem.libretexts.org/Bookshelves/Physical_and_Theoretical_Chemistry_Textbook_Maps/Supplemental_Modules_\(Physical_and_Theoretical_Chemistry\)/Spectroscopy/Electronic_Spectroscopy/Selection_Rules_for_Electronic_Spectra_of_Transition_Metal_Complexes](https://chem.libretexts.org/Bookshelves/Physical_and_Theoretical_Chemistry_Textbook_Maps/Supplemental_Modules_(Physical_and_Theoretical_Chemistry)/Spectroscopy/Electronic_Spectroscopy/Selection_Rules_for_Electronic_Spectra_of_Transition_Metal_Complexes)
- Lancashire, R. J. *LibreTexts™* (2020). *Magnetic Moments of Transition Metals*. <https://chem.libretexts.org/@go/page/19707> [accessed 15 December 2021].
- Lever, A. B. P., & Mantovani, E. (2011). Isotopic Studies of the Metal–Ligand Bond. Part III. The Far Infrared Spectra of Some Tetragonal Diamine Complexes of Cobalt(II) and Nickel(II): Studies of the Metal–Nitrogen Bond, as a Function of Metal Ion and of Spin State, *Canadian Journal of Chemistry*, *51*(10):1567-1581. DOI:10.1139/v73-237
- LibreTexts™ (2020). *Magnetism*. <https://chem.libretexts.org/@go/page/263246>. [accessed 15 December 2021]
- Mihsen, H. H., & Shareef, N. K. (2018). Synthesis, Characterization of Mixed- ligand Ccomplexes Containing 2,2-Bipyridine and 3-aminopropyltriethoxysilane. *Journal of Physics: Conference Series*, *1032*, 012066. doi:10.1088/1742-6596/1032/1/012066.
- Mir, M.A., & Ashraf, M. W. (2021), TG, DTA Pyrolytic Analysis of Cobalt, Nickel, Copper, Zinc, and 5,8-Dihydroxy-1,4-Naphthoquinone Chelate Complexes, *Hindawi Journal of Chemistry*, 1-13. <https://doi.org/10.1155/2021/6691137>
- Oswole, A. A., Kolawole, G. A., & Fagade, O. E. (2008). Synthesis, characterization and biological studies on unsymmetrical Schiff-base complexes of nickel(II), copper(II) and zinc(II) and adducts with 2,2'-dipyridine and 1,10-phenanthroline, *Journal of Coordination Chemistry*, *61* (7), 1046–1055.
- Paswan, S., Anjum, A., Singh, A. P., & Dubey, R. K. (2019). Synthesis and Spectroscopic Characterization of Lanthanide Complexes Derived from 9,10-Phenanthrenequinone And Schiff Base Ligands Containing N, O Donor Atoms. *Indian Journal of Chemistry*, *58A*(4), 446-453.
- Pathshala (2021). *Inorganic Chemistry-II: Metal-Ligand Bonding, Electronic Spectra and Magnetic Properties of Transition Metal Complexes*. http://meerutcollege.org/mcm_admin/upload/1588000002.pdf. [accessed 15 December 2021]
- Rastina, Sudarwanto, M., & Wientarsih, I. (2015). Antibacterial Activity of Ethanol Extract of Curry Leaf (*Murraya koenigii*) on *Staphylococcus aureus*, *Escherichia coli*, and *Pseudomonas Sp.* *Jurnal Kedokteran Hewan (Indonesian Journal of Veterinary Sciences)*, *9*(2), 185-188.
- Shad, H. A., Thebo, K. H., Ibupoto, Z. H., Malik, M. A., O'Brien, P., & Raftery, J. (2011). Synthesis, characterization, and crystal structure of a copper(II) complex of 1,10-phenanthroline and succinate, *Journal of Coordination Chemistry*, *64*(13), 2353-2360. DOI 10.1080/00958972.2011.595789.
- Singh, B. K., Mishra, P., Prakash, A., & Bhojak, N. (2017). Spectroscopic, electrochemical and biological studies of the metal complexes of the Schiff base derived from pyrrole-2-carbaldehyde and ethylenediamine, *Arabic Journal of Chemistry*, *10*(2), S472-S483. <http://dx.doi.org/10.1016/j.arabjc.2012.10.007>
- Skyrianou, K. C., Perdih, F., Turel, I., Kessissoglou, D. P., & Psomas, G. (2010). Nickel–quinolones interaction. Part 2 – Interaction of nickel(II) with the antibacterial drug oxolinic acid, *Journal of Inorganic Biochemistry*, *104* (2), 161–170. <https://doi.org/10.1016/j.jinorgbio.2009.10.017>

- Sondavid, N., Shweta, B., Bryan, W., Joung, C., Naresh, T., & Jun, K. H. (2020). Cobalt(II) Benzazole Derivative Complexes: Synthesis, Characterization, Antibacterial and Synergistic Activity. *ChemistrySelect*, 5, 3471-3476. DOI:10.1002/slct.202000222.
- Sugiyarto, K. H., Kusumawardani, C., & Wulandari, K. E. (2018). Synthesis and Structural Analysis of Powder Complex of Tris(bipyridine)cobalt(II) trifluoromethanesulfonate Octahydrate, *Indonesian Journal of Chemistry*, 18 (4), 696 - 701. DOI: 10.22146/ijc.26833
- Sugiyarto, K. H., Kusumawardani, C., Sutrisno, H., & Wibowo, M. W. A. (2018). Structural Analysis of Powdered Manganese(II) of 1,10-Phenanthroline (phen) as Ligand and Trifluoroacetate (TFA) as Counter Anion. *Oriental Journal of Chemistry*, 34(2), 735-742. DOI:10.13005/ojc/340216
- Sugiyarto, K. H., Louise, I. S. Y., & Wilujeng, S. S. (2020). Preparation and Powder XRD Analysis of Tris(2,2'-bipyridine)nickel(II) Trifluoroacetate. *Indonesian Journal of Chemistry*, 20(4), 833 - 841. DOI: 10.22146/ijc.46483
- Sugiyarto, K. H., Marini, D. W., Sutrisno, H., Purwaningsih, D., & Kusumawardani, C. (2023). Synthesis of Powdered $[Mn(bipy)_3](CF_3SO_3)_2 \cdot 5.5H_2O$: The Physical Properties and Antibacterial Activity. *Indonesian Journal of Chemistry*, 23 (1), 242 - 250. DOI: 10.22146/ijc.77565.
- Sugiyarto, K. H., Saputra, H. W., Permanasari, L., & Kusumawardani, C. (2017). Structural analysis of powder complex of $[Mn(phen)_3](CF_3SO_3)_2 \cdot 6.5H_2O$, *AIP Conference Proceedings* 1847, 040006-1-040006-7. DOI: 10.1063/1.4983902. <http://dx.doi.org/10.1063/1.4983902>.
- Sutrisno, H., Kusumawardani, C., Rananggana, R. Y., & Sugiyarto, K. H. (2018). Structural Analysis of Powder Tris(phenanthroline)nickel(II) Trifluoroacetate, *Chiang Mai Journal of Science*, 45(7), 2768-2778. <http://epg.science.cmu.ac.th/ejournal/>
- Suzuki, H., Takiguchi, T., & Kawasaki, Y. (1978). Synthesis and spectroscopy of acetato and dithiocarbamate complexes of bis(cyclopentadienyl) zirconium(IV), *Bulletine of the Chemical Society of Japan*, 51 (6), 1764-1767.
- Tosoniani, S., Ruiz, C. J., Rios, A., Frias, E., & Eichler, J. F. (2013). Synthesis, characterization, and stability of iron (III) complex ions possessing phenanthroline-based ligands, *Open Journal Inorganic Chemistry*, 3 (1), 7-13. DOI:10.4236/ojic.2013.31002
- Uddin, S., Hossain, Md. S., Latif, Md. A., Karim, Md. R., Mohapatra, R. K., & Zahan, Md. K-E. (2019). Antimicrobial Activity of Mn Complexes Incorporating Schiff Bases: A Short Review. *American Journal of Heterocyclic Chemistry*, 5(2), 27-36. DOI: 10.11648/j.ajhc.20190502.12.
- Yao, J. C., Ma, L. F., & Yao, F. J. (2005). Crystal structure of tris(2,2'-bipyridine)cobalt(II)diperchlorate, $[Co(C_{10}H_8N_2)_3][ClO_4]_2$. *Zeitschrift Für Kristallographie, New Crystal Structures*, 220(3): 483-484. doi:10.1524/ncrs.2005.220.3.483.
- Zhou, Y., Li, X., Xu, Y., Cao, R., & Hong, M. (2003). Tris(2,2'-bipyridine)nickel(II) perchlorate, *Acta Crystallography, Section E: Structure Report Online*, 59 (5), m300-m302.